Association Complex Formation in Gas-Phase Ta Cluster Reactions with Simple Alkanes: Probing the Role of Entropy in Rate Determination for Barrierless Adsorption Processes

David B. Pedersen, J. Mark Parnis,* and Rick D. Lafleur

Department of Chemistry, Queen's University, Kingston, Ontario K7L 3N6, Canada, and Department of Chemistry, Trent University, Peterborough, Ontario K9J 7B8, Canada

David M. Rayner

Steacie Institute for Molecular Sciences, National Research Council of Canada, 100 Sussex Drive, Ottawa, Ontario K1A OR6, Canada

Received: October 1, 2003; In Final Form: February 1, 2004

Rate coefficients for the reactions of ethane, propane, *n*-butane, isobutane, and neopentane with Ta atoms and Ta clusters consisting of up to 30 Ta atoms have been measured in a fast-flow reactor. A near-monotonic dependency of the rate coefficients on cluster size is observed for each of these hydrocarbons, with the exception of Ta_{11}, which exhibits rate coefficients that are several times that observed for the analogous reaction with Ta_{10} and Ta_{12}, for propane, *n*-butane, and isobutane. Modeling the general trend in the rate coefficients using transition state theory is found to require a relatively loose transition state with free rotation of the hydrocarbon about the bonding point on the cluster, consistent with the rate-determining step being cluster removal by an association reaction process. It is demonstrated that, in general, metal cluster reactions with reagents that can form strongly bound association complexes may exhibit little evidence of cluster-size-based selectivity in the rate of cluster removal, despite exhibiting significant selectivity in terms of the extent of the dehydrogenation reaction involved.

I. Introduction

A central research focus in metal cluster chemistry is the investigation of cluster size specific reactivity, and the underlying factors that control such selectivity. To this end, molecular surface scientists have focused on correlations between cluster electronic and local geometric structures and cluster size-dependent reactivity.[1,2] However, not all cluster reactions show size dependence in the rate of cluster removal. For example, the reaction of Nb clusters with isobutane[3] exhibits a near-monotonic increase in cluster removal rate with cluster size, despite significant variations in the extent of hydrogen loss with cluster size. We have now determined that, with a few exceptions, nonselectivity in the rate of cluster removal is generally observed with other early transition metal clusters and hydrocarbons, including Ta clusters for which data are presented here. This general lack of size selectivity presents a significant new challenge to the interpretation of metal cluster reaction kinetics. We offer here an explanation based upon transition-state theory analysis of the reaction rate coefficient trends, demonstrating that the reaction kinetics data are most consistent with a barrierless association complex formation process.

Barrierless molecular adsorption processes are ubiquitous precursors to chemisorption on transition metal surfaces and are generally assumed to occur with near-unit probability.[4] A sticking probability of 1.0 assumes that, in lieu of an activation energy barrier, the enthalpy-derived Gibbs free energy gain associated with adsorption of molecules is much greater than the entropy-derived Gibbs free energy loss incurred, and the adsorption process effectively amounts to uninhibited descent into the potential energy well associated with the molecule in the adsorbed state. Accordingly, double- or triple-well potential energy curves representing progress along the reaction coordinate from free molecule to chemisorbed states are commonly assumed for such processes.[4] From a reaction kinetics perspective, free energy curves are more relevant, as they account for the change in both enthalpy *and* entropy, both of which significantly affect the reaction rate. For relatively large reagents, loss of translational and rotational degrees of freedom upon adsorption amount to large losses in entropy that must be explicitly considered when modeling the reaction rate.

Some time ago, Gilbert and co-workers[5] applied variational transition state theory for a model metal surface system and predicted that, in some cases, entropic constraints associated with adsorption can dominate and determine the adsorption rate. They associate the loss of entropy with Gibbs free energy barriers that restrict motion of the adsorbate over the metal surface. Extrapolating from this concept as the size and mass of the reagent increases, entropy associated with translation and rotation of the free reagent increases, as does the entropy loss on adsorption. Accordingly, for large, heavy reagents that interact weakly with the metal surface, the loss of entropy upon adsorption may make a contribution to the Gibbs free energy that exceeds that of the exothermicity of metal−reagent binding. In this case, the entropy loss gives rise to a Gibbs free-energy barrier to adsorption, the apex of which constitutes a well-defined transition state. The reactions of hydrocarbons with transition metal clusters represent such a case and offer an opportunity to quantify the influence of entropy on the rate of such barrierless adsorption reactions. Flow-tube reactors, equipped with laser ablation sources, provide a convenient vehicle for the study of reactivity of metal clusters under well-defined temperatures and pressures, yielding absolute reaction rate

10.1021/jp036942i CCC: $27.50
Published on Web 03/13/2004

coefficients that are amenable to quantitative theoretical interpretation and analysis. To the extent that behavior of metal clusters corresponds to that of portions of metal surfaces, such systems may be used to study metal surface−molecule interactions in great detail. This approach has been used to establish structure-dependent reactivity as a paradigm in the field of cluster science.[1,6−16] However, for classes of cluster reactions that show little size dependence in the rate of cluster removal, the cluster/flow system approach affords an opportunity to systematically vary cluster mass and corresponding number of constituent atoms, to determine the effect of these parameters on the reaction rate. In addition, working with a family of chemically similar molecules differing principally in terms of their size and entropy offers an opportunity to directly probe the role of entropy in determining reaction rate for barrierless cluster reactions.

Of the diatomics, CO and O_2 are the only known species to display nonselective reactivity.[1,13,16] The absence of any significant potential energy barrier to reaction is thought to distinguish the CO and O_2 reactions from those of other diatomics. The temperature independence of the Nb_n−isobutane rate coefficients exemplifies the absence of a significant activation energy barrier in metal cluster−hydrocarbon reactions. The rate coefficients associated with these structure-insensitive reactions constitute valuable data sets for the establishment of appropriate reactivity models for such barrierless reaction processes. Previous work by our group has shown that cluster structure-insensitive reactions can, in some cases, be modeled using simple collision theory. Rate coefficients for the reactions of Nb clusters with isobutane have been modeled in this way.[3] The success of the model indicates that the physical size of clusters, or some other extensive cluster property, plays a major role in determining rates of reactions in nonactivated systems. In more recent work, we have discussed the implications that cluster polarizability has on reactivity in determining the collision rate and the stability of physisorbed precursor states, which serve as intermediates in many cluster reactions.[17] In the Nb_n−isobutane reaction the rates of reaction lie in the 10^{-13} to 10^{-12} cm^3 s^{-1} range, 2−3 orders of magnitude below the expected collision rate. In the absence of any significant activation energy barrier, the relatively slow rate of reaction can only be explained in terms of entropic considerations, similar to those predicted by Gilbert and co-workers,[5] as is developed below in detail.

Studies of cluster depletion kinetics have culminated in the general application of double-well models of the reaction path potential energy profile.[2] In this context, reactions are assumed to involve initial molecular adsorption, followed by dissociative adsorption (chemisorption), as shown in Figure 1. We demonstrate here that application of transition state theory (TST) clearly indicates that the removal of Ta clusters by hydrocarbons proceeds via a molecular association complex formation step. Previous work suggests that for metal cluster reactions, a combination of strong dispersive forces, dative bonding, and agostic-type interactions may result in relatively strongly bound association complexes to which significant depletion of the bare cluster may be attributed. Accordingly, it is not clear whether the rate of cluster depletion observed in metal cluster depletion kinetics reflects the nature of the transition state to formation of the molecularly adsorbed species (TS1), or to that of the transition state to dissociative chemisorption (TS2). It is the purpose of the present work to demonstrate that application of TST can be a useful tool in making this distinction, and that the entropy loss associated with the formation of a molecular adsorption transition state is the primary determinant of the magnitude of the cluster removal rate coefficients.

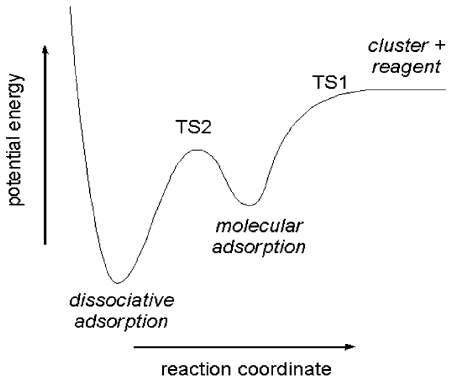

Figure 1. Schematic double-well potential energy curve for a metal cluster−molecule reaction. The location of the transition states for molecular adsorption (TS 1) and dissociative adsorption (TS 2) are noted.

II. Experimental Section

The apparatus in the two configurations used in this work has been described in detail[3,17] and therefore only a brief description is given here. Clusters are generated using a Smalley-type laser ablation source. A pulsed XeCl laser is focused onto a translating and rotating metal rod, over which a 15 000 standard cubic centimeter continuous flow of He (99.995% pure from Liquid Carbonics Inc.) is maintained, generating a metallic plasma entrained in the He flow. The He-plasma gas flows through a 1 cm long, 0.2 cm diameter channel, where clusters are formed. Subsequently, the mixture expands into the large-bore (7.3 cm in diameter) flow tube reactor. In the presence of excess He bath gas the clusters rapidly equilibrate to flow tube temperature and pressure conditions.[12]

Flow tube pressure is varied in the range 0.5−2.2 Torr by partially closing the gate valve to the vacuum (600 L s^{-1} Edwards EH2600 Roots blower backed by an Edwards E1M275 mechanical pump). Data were collected at various fixed temperatures between 270 and 375 K, and at constant pressures ranging from 0.5 to 2.2 Torr. The specific temperature and pressure conditions used with particular gases are noted below.

The hydrocarbon reagent gases ethane (Matheson Research Grade 99.9%), propane (Matheson Instrument Grade 99.98%), *n*-butane (Matheson Research Grade 99.995%), isobutane (Matheson Instrument Grade 99.5%), and neopentane (Matheson Research Grade 99.87%) are introduced through a shower-head inlet 60.6 cm downstream from the cluster source. Reagent gas pressures in the reactor are controlled by a mass flow controller (MKS model 1159). On reaching the end of the flow tube, the clusters and their reaction products pass into either an on-axis time-of-flight (*n*-butane, isobutane, neopentane) or a reflectron time-of-flight (ethane, propane) mass spectrometer (TOFMS) situated perpendicular to the flow tube axis. A pressure drop of approximately 6 orders of magnitude is maintained between the TOFMS and the flow tube by differential pumping, using an Edwards Diffstak 2300 L s^{-1} diffusion pump and an Edwards Diffstak 800 L s^{-1} diffusion pump in conjunction with an electromagnetic shutter used to reduce gas load. Clusters and reaction products entering the TOFMS are photoionized[18] by a pulsed ArF laser operating at 193 nm that is triggered at a set delay with respect to firing of the ablation laser. The detector signal is digitized and sent to a personal computer for analysis. All mass spectra collected were averaged 200 times. Note that, in the case of Ta atoms, detection of the ground-state atom is

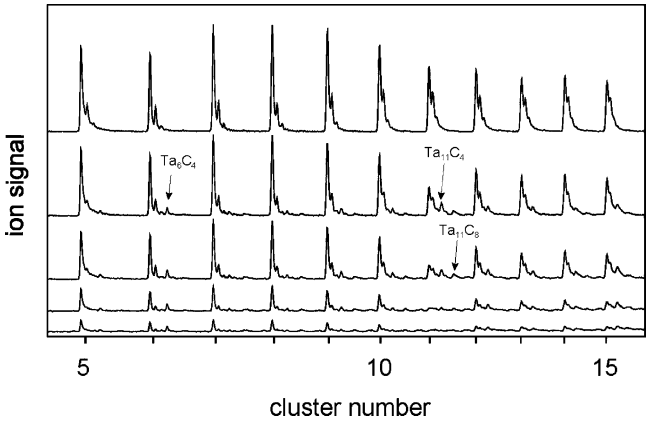

Figure 2. Mass spectra of Ta_5-Ta_{15} showing the effect of introducing isobutane into the flow tube. Reagent flow increases with descending spectral order, from 0 (top spectrum) to 80 (bottom spectrum) sccm. Product peaks associated with Ta_6 and Ta_{11} are noted, with their empirical formula for the peak center mass.

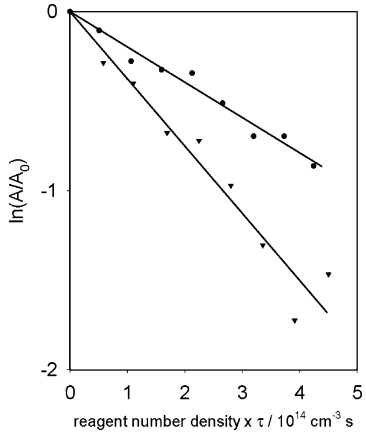

Figure 3. Representative pseudo-first-order kinetics plots used to determine absolute second-order rate coefficients for Ta_n reactions with alkanes. Illustrated are data for Ta_{18} with propane (top trace) and Ta_{10} with isobutane (bottom trace).

not possible as a one-photon ionization process. Therefore, kinetics associated with Ta atoms reported here are likely due to ionization and detection of metastable excited-state Ta atoms.

III. Results

Ta atoms and clusters were observed to react with all alkanes studied, i.e., ethane, propane, *n*-butane, isobutane, and neopentane. Representative mass spectra are shown in Figure 2 for data collected at 1 Torr total pressure with isobutane. Introduction of any of the alkanes in the reaction zone caused depletion of bare Ta atoms or clusters. In the case of isobutane, product peaks reflecting sequential addition of significantly dehydrogenated isobutane can be clearly seen. Figure 2 shows the sequential growth of two products on Ta_{11}, for which the mass of these product peaks at the maximum value corresponds to production of $Ta_{11}C_4$ and $Ta_{11}C_8$, respectively. Many other Ta clusters yield addition of C_4 units as products in similar processes, although our resolution does not allow us to rule out the production of some C_4H_2 or even C_4H_4 as addition products in many cases. With most other alkanes studied, product features were not visible, likely due to low ionization efficiency. No dehydrogenation is evident in the reaction with neopentane, although extensive rearrangement of the hydrocarbon backbone is clearly present, because product masses show sequential addition of units of 15 (CH_3). For the products that are observed, the occurrence of postionization dehydrogenation cannot be ruled out in light of the fact that atomic Ta ions are known to dehydrogenate hydrocarbons.[19]

By monitoring the rate of atom or cluster depletion as a function of reagent partial pressure, one may obtain absolute second-order rate coefficients. Assuming that the reagent gas is in sufficient excess, the pseudo-first-order kinetics expression appropriate for atom or cluster depletion is

$$\ln\left(\frac{A}{A_0}\right) = -k^{(2)}P_{\text{alkane}}\tau \qquad (1)$$

where A and A_0 are the mass spectral peak areas in the presence and absence of reagent gas, respectively, P_{alkane} is the reagent partial pressure in the flow tube, τ is the reactant contact time, and $k^{(2)}$ is the absolute second-order rate coefficient. All pseudo-first-order kinetics plots were linear, as typified in Figure 3 by the reactions of Ta_{18} with propane and Ta_{10} with isobutane. The rate coefficients calculated from the slopes of such plots for Ta atoms and clusters are presented in Table 1 and plotted in Figures 4−7.

All alkanes studied show a generally smooth increases in the rate coefficients as the number of constituent Ta atoms increases. Exceptions to this trend are the slightly elevated rates observed in general for the Ta atom, Ta_2 and Ta_3, as well as the anomalously high rate coefficients observed with Ta_{11} for all gases having secondary or tertiary C−H bonds (2−10-fold increase). One specific exception is an increase in rate observed with *n*-butane only for Ta_{23} and Ta_{27} (2−3-fold increase). Other deviations are generally modest and much smaller than that typically observed with reagents such as H_2, for which variations of several orders of magnitude have been found.[2] The extent of cluster depletions, and hence the rate coefficients determined, were not sensitive to ionization laser fluences, indicating that the experiments were conducted under conditions of single-photon ionization. Rate coefficients showed no obvious dependence on total flow tube pressure between 0.5 and 3 Torr, as demonstrated by the representative data given for neopentane at 1 and 2 Torr in Table 1. Data recorded at various temperatures with ethane, propane, and isobutane also showed no significant or systematic effect on rate coefficients, as demonstrated by representative data for ethane and isobutane in Table 1. Data for the isobutane reaction with Nb_{11} only showed significant inverse temperature dependence and allowed a crude estimate of the Arrhenius activation energy for the rate-determining step, for which we obtain -6 kJ mol^{-1}, likely reflecting a reversible complexation or reaction process. This, and the unusually fast reaction of this cluster, indicates that removal of Ta_{11} is due to a mechanism that is distinct with respect to all other clusters studied.

IV. Discussion

A. Early Transition Metal Cluster-Alkane Rate Coefficients. The results given above demonstrate that Ta cluster reactions with a number of small alkanes generally show no cluster size selectivity beyond a slow monotonic increase in rate coefficient with cluster size, with a few notable exceptions such as Ta_{11}. In addition to the above results, experiments by Hamrick and Morse also found the relative rates of Ta cluster reactions with ethane to increase weakly, but smoothly with cluster size.[9] Lafleur et al. observed smooth increases in rate coefficients for Nb cluster reactions with isobutane.[3] Near-monotonic, modest increases in rate coefficients with increasing cluster size therefore appear to be characteristic of alkane

TABLE 1: Absolute Second-Order Rate Coefficients $k^{(2)}$ for the Removal of Ta_n by Alkanes in Units of 10^{-12} cm^3 s^{-1}, under Various Pressure and Temperature Conditions

	n-butane	neopentane		isobutane			ethane		propane
N	$P = 2$ Torr, $T = 300$ K	$P = 1$ Torr, $T = 302$ K	$P = 2$ Torr, $T = 302$ K	$P = 1$ Torr, $T = 372$ K	$P = 1$ Torr, $T = 300$ K	$P = 1$ Torr, $T = 278$ K	$P = 1$ Torr, $T = 300$ K	$P = 1$ Torr, $T = 347$ K	$P = 1$ Torr, $T = 298$ K
1	0.45 (11)	2.0 (6)	2.0 (3)	3.4 (5)	3.1 (2)	3.0 (4)	0.25 (11)	0.26 (15)	0.24 (27)
2	0.63 (6)	1.9 (7)	2.5 (3)	3.8 (3)	3.6 (3)	4.9 (6)	0.27 (10)	0.26 (12)	0.29 (21)
3	0.71 (9)	2.5 (6)	3.1 (3)	3.8 (2)	4.0 (2)	4.5 (2)	0.31 (9)	0.31 (14)	0.38 (10)
4	0.15 (9)	2.0 (9)	2.9 (4)	3.2 (2)	3.3 (2)	3.1 (3)	0.18 (13)	0.14 (30)	0.14 (18)
5	0.17 (9)	2.6 (7)	3.4 (3)	3.5 (2)	3.7 (2)	3.8 (3)	0.22 (11)	0.26 (15)	0.15 (17)
6	0.18 (8)	3.1 (7)	3.8 (3)	3.8 (1)	4.0 (3)	4.3 (3)	0.30 (12)	0.35 (17)	0.20 (13)
7	0.15 (5)	4.0 (9)	3.9 (3)	4.0 (1)	4.1 (3)	4.3 (4)	0.29 (15)	0.27 (16)	0.19 (20)
8	0.17 (6)	3.4 (8)	4.1 (3)	4.0 (2)	4.3 (3)	4.4 (3)	0.34 (15)	0.40 (14)	0.22 (16)
9	0.22 (7)	3.9 (8)	4.7 (3)	4.5 (2)	4.7 (3)	5.0 (4)	0.43 (10)	0.47 (19)	0.26 (13)
10	0.27 (11)	3.9 (9)	5.0 (4)	4.6 (2)	5.0 (3)	5.3 (3)	0.32 (12)	0.42 (26)	0.33 (12)
11	4 (18)	5.5 (7)	5.8 (3)	6.3 (2)	9.8 (1)	12.5 (4)	0.62 (12)	0.69 (24)	1.1 (7)
12	0.22 (8)	5.4 (8)	5.1 (5)	5.2 (2)	5.1 (3)	5.7 (4)	0.61 (10)	0.72 (16)	0.47 (12)
13	0.33 (5)	6.1 (8)	6.6 (5)	5.3 (2)	5.2 (2)	5.8 (4)	0.86 (14)	0.82 (19)	0.52 (17)
14	0.21 (8)	5.8 (9)	6.4 (2)	5.1 (3)	5.3 (3)	5.8 (5)	0.71 (11)	0.93 (11)	0.57 (12)
15	0.27 (7)	5.7 (9)	5.8 (4)	5.4 (3)	5.3 (2)	5.7 (5)	0.71 (7)	1.1 (20)	0.59 (13)
16	0.21 (10)	5.4 (9)	4.8 (4)	5.6 (2)	5.5 (2)	6.3 (5)	0.81 (9)	1.1 (23)	0.72 (13)
17	0.20 (10)	5.4 (10)	6.8 (8)	5.7 (2)	5.8 (3)	6.7 (5)			0.76 (16)
18	0.20 (10)	5.6 (9)	6.4 (4)	5.5 (3)	5.8 (3)	6.6 (6)			0.75 (17)
19	0.22 (10)	5.5 (10)	7.2 (6)	5.5 (2)	5.9 (3)	6.5 (6)			0.87 (13)
20	0.32 (8)	6.3 (9)	6.4 (4)	5.6 (4)	5.6 (3)	6.1 (5)			0.97 (13)
21	0.41 (7)	6.4 (9)	7.7 (4)	5.7 (3)	5.5 (4)	5.7 (5)			1.0 (12)
22	0.16 (14)	5.7 (12)	6.3 (4)	5.4 (5)	5.8 (3)	6.0 (5)			0.95 (14)
23	0.80 (5)	7.7 (10)	8.3 (3)	6.0 (3)	7.0 (5)	6.9 (6)			1.2 (14)
24	0.26 (11)	6.1 (11)	7.8 (2)	6.1 (3)	6.2 (3)	6.8 (6)			1.1 (17)
25	0.40 (8)	5.8 (14)	8.9 (3)	7.0 (2)	6.6 (3)	6.2 (6)			1.0 (21)
26	0.48 (7)	7.5 (12)	8.3 (2)	5.9 (4)	6.3 (3)	6.3 (5)			1.5 (19)
27	1.4 (5)	8.9 (10)	7.7 (6)	6.8 (4)	6.8 (3)	7.7 (6)			1.6 (17)
28	0.39 (9)	5.2 (13)	7.3 (5)	5.8 (4)	5.8 (3)	5.9 (5)			1.3 (24)
29	0.28 (10)	6.9 (11)	8.3 (4)	6.7 (5)	5.8 (2)	5.6 (5)			1.4 (18)
30	0.49 (7)	6.3 (15)	8.8 (3)	6.7 (5)	6.3 (4)	8.4 (8)			

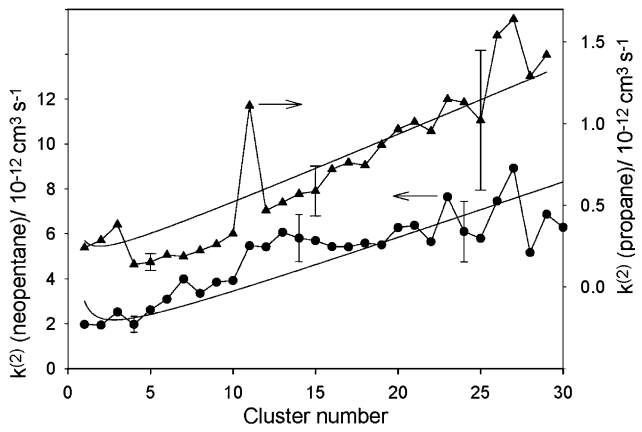

Figure 4. Rate coefficients for the reactions of Ta_n with propane (upper data) and neopentane (lower data) plotted as functions of the number of Ta atoms per cluster. Error bars reflect the estimated 20% average uncertainty in the precision of the measurements. One-variable fits to the data using the transition-state theory model are shown as solid lines.

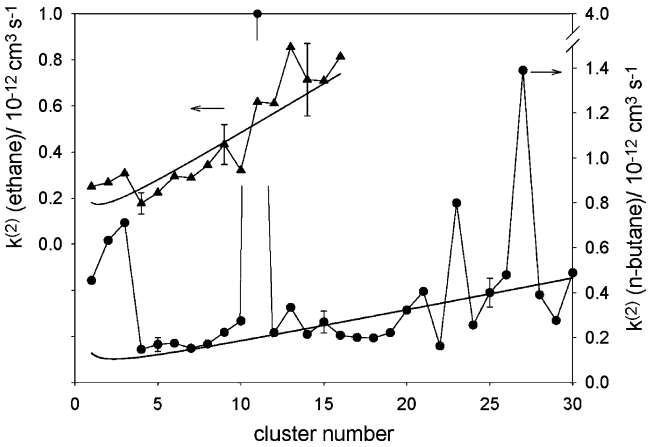

Figure 5. Rate coefficients for the reactions of Ta_n with *n*-butane (lower data) and ethane (upper data) plotted as functions of the number of Ta atoms per cluster. Error bars reflect the estimated 20% average uncertainty in the precision of the measurements. One-variable fits to the data using the transition-state theory model are shown as solid lines.

reactions with early transition-metal clusters. This reactivity characteristic contrasts sharply with the observation that such clusters may exhibit marked cluster size selectivity in the extent to which they undergo subsequent chemical transformations, as is demonstrated by the variation in degree of dehydrogenation in the Nb cluster/isobutane work. The ionization potentials of Ta clusters are known to fluctuate with size[20] and there is no reason to expect small transition metal clusters to present reaction sites whose geometries are independent of cluster size. An exception might be when the reactive site is a single constituent atom, and the reaction is very insensitive to the influence of metal−metal bonding on that atom.

B. Transition State Theory Analysis of the Rate Coefficients. The measurement of absolute rate coefficients at well-defined temperatures and pressures allows us to gain insight into the character of the transition state, and therefore the nature of the rate-determining step, through the application of TST. We present the following analysis to allow us to distinguish between formation of a molecular association complex and a direct, barrierless dissociative adsorption process. Application of TST also helps to explain the absence of cluster size selectivity in the rate data.

For a barrierless reaction, $k^{(2)}$ is given by the transition state expression:

$$k^{(2)} = \frac{\sigma k_B T}{h} \times \frac{Q_{tot}^{\ddagger}}{Q_{tot}^{cluster} Q_{tot}^{alkane}} \qquad (2)$$

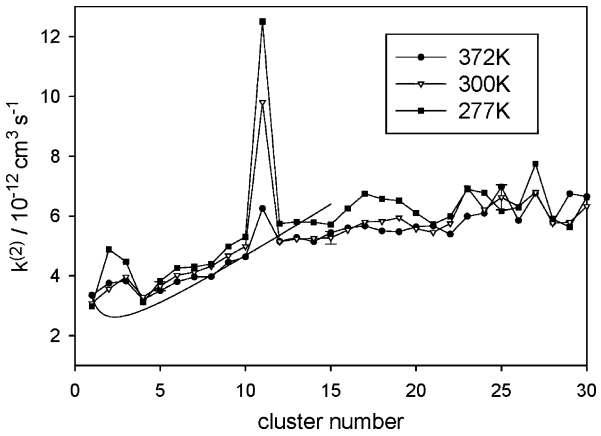

Figure 6. Rate coefficients for the reactions of Ta_n with isobutane plotted as functions of the number of Ta atoms per cluster, at three different flow tube temperatures (■ = 277 K, ∇ = 300 K, ● = 372 K). A one-variable fit to the data using the transition-state theory model is shown as a solid line.

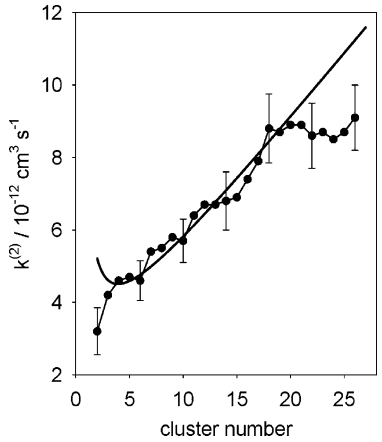

Figure 7. Rate coefficients of Lafleur et al.[3] for the reactions of Nb_n with isobutane plotted as a function of the number of Nb atoms per cluster. Error bars reflect the estimated 20% average uncertainty in the precision of the measurements. A one-variable fit to the data using the transition-state theory model is shown as a solid line.

Here, $Q_{tot}^{\ddagger}$, Q_{tot}^{alkane}, and $Q_{tot}^{cluster}$ are the total partition functions for the reaction transition state, alkane, and Ta cluster, respectively, k_B is Boltzmann's constant, T is absolute temperature, h is Planck's constant, and σ is the reaction path degeneracy. The partition functions for the reactants and σ can be estimated so that $Q_{tot}^{\ddagger}$ is the only unknown quantity. The partition function, $Q_{tot}^{\ddagger}$, is a measure of the tightness of the transition state and has mechanistic implications (see below).

Equation 7 was used to model rate coefficients for clusters of different sizes for each of the four hydrocarbons in question at a temperature of 300 K, following estimation of the necessary partition functions using several approximations.[21] The cluster was treated as a solid sphere, the alkane as a symmetric rotor, and the transition state as a loosely associated complex in which the alkane is bonded to the cluster surface at a single point. The alkane was fixed at a distance of 2 Å from the cluster surface. All cluster atoms were assumed to be available reaction sites within the cluster size range considered. The vibrational frequencies of all cluster and hydrocarbon modes were assumed to be preserved upon complexation. Four new intramolecular cluster-hydrocarbon complex vibrational modes arise as a result of loss of translational and rotational degrees of freedom (excluding the reaction coordinate). The contribution from these new modes to $Q_{vib}^{\ddagger}$ is expressed as $Q_{vib}{}'^{\ddagger}$. To obtain an acceptable fit to the experimental data, free rotation about the cluster−alkane reaction coordinate was found to be required in the model. The experimental rate coefficients were fit by optimizing the value of $Q_{vib}{}'^{\ddagger}$, the only variable parameter in our model. We find the best fit of the experimental data to be obtained with the values of $Q_{vib}{}'^{\ddagger}$ given in Table 2, which vary over 2 orders of magnitude from 368 (ethane) to 3.53×10^4 (neopentane). Note that the variation in this ratio is only associated with the choice of hydrocarbon, because all aspects of the cluster contributions to the overall calculation are held constant over all hydrocarbons studied.

TABLE 2: Summary of Parameters Obtained from TST Fit of Experimental Data for Kinetics of Ta Cluster Removal by Various Hydrocarbons[a]

	$Q_{vib}{}'^{\ddagger}$	$\bar{\nu}$/cm^{-1}	$\Delta_r S^{\ddagger}$/J K^{-1} mol^{-1}
ethane	368.5	54	−107 to −90
propane	1495	36.5	−104 to −91
n-butane	1695	35.3	−111 to −100
isobutane	27720	16.8	−85 to −73
neopentane	35300	15.8	−87 to −75

[a] Entropy of activation range corresponds to the range of values obtained for the clusters studied.

The optimal values obtained for $Q_{vib}{}'^{\ddagger}$ may be further characterized by means of an effective or average vibrational wavenumber $\bar{\nu}_{eff}$, associated with the four new vibrational modes generated on formation of the transition state. This may be done by assuming that all four new modes are degenerate, and solving for $\bar{\nu}_{eff}$ in the expression for the contribution of these modes to the transition state partition function:

$$Q_{vib}{}'^{\ddagger} = \left(\frac{1}{\left(1 - \exp\left(\frac{hc\bar{\nu}_{eff}}{k_B T}\right)\right)^4} \right) \qquad (3)$$

It is recognized that this method of characterization of the transition state is not expected to accurately predict individual vibration wavenumbers for new modes generated on formation of the transition state. Nonetheless, such an approach offers a useful and more tangible approach to the characterization of the contribution to the vibrational partition function made by $Q_{vib}{}'^{\ddagger}$. Values for the effective vibrational wavenumber $\bar{\nu}_{eff}$ for the new transition state modes are given for each alkane studied in Table 2 and range from 54 (ethane) to 15.8 cm^{-1} (neopentane). The variation obtained for this parameter reflects a dependence upon the mass of the alkane involved and shows a roughly inverse square root dependence on mass of the alkane, as might be expected for a system that can be crudely described as an alkane moving in harmonic motion with respect to a massive and relatively immobile cluster. If this system were treated as a pseudodiatomic molecule, the reduced mass involved would then be essentially equal to the mass of the alkane, and the vibrational wavenumber associated with it would scale with the inverse square root of this quantity, as seen here.

The resulting optimized TST rate coefficients are plotted in Figures 4−7 along with the experimentally determined rate coefficients. In general, the model satisfactorily describes the overall trend and magnitude of the rate coefficients as a function of n for the small clusters studied with ethane, propane, *n*-butane, and neopentane. Notable, however, is the failure of the model to account for the lack of significant variation in the rate coefficients for Ta_{15}−Ta_{30} (isobutane), and the clusters with consistently high rate coefficients with all alkanes studied, such as Ta, Ta_2, and Ta_3, and those that give anomalous behavior with isobutane noted above. Nonetheless, it is a significant

achievement that a one-parameter model can account for the general variation in rate coefficients for all alkanes studied, implying that most clusters are reacting via a similar transition state morphology and reaction mechanism.

As a further test of this model, the rate coefficients of Lafleur et al. for the reaction of Nb_n with isobutane[3] were also modeled, as shown in Figure 7. Here the best value of $Q_{vib}^{\ddagger}$ was found to be 2.23×10^4 with a corresponding value of $\bar{\nu}_{eff} = 16.8$ cm^{-1}. These values are very close to those calculated for the Ta_n−alkane reactions. At higher *n* the model deviates from the actual trend in the rate coefficients, in a manner similar to that noted above for Ta clusters with isobutane. For the smaller Nb clusters, however, the model satisfactorily depicts the trend and the absolute value of the experimental rate coefficients.

C. Entropy Loss as Rate Determinant in Molecular Association Complex Formation Processes. Transition state modeling of all alkane reactions discussed here was done with a transition state model characterized by free internal rotation of the alkane in the complex, conserved vibrational modes in the cluster and hydrocarbon, and a low value of $Q_{vib}^{\ddagger}$. Together, these characteristics imply that the appropriate transition state for the rate-determining step is relatively "loose", in the chemical kinetics sense. It is noteworthy that choice of transition-state parameters that reflect a relatively "tight" transition state, such as removing the free rotation of the hydrocarbon, or increasing the effective vibrational wavenumbers of the new vibrational modes of the transition state by a modest 20%, resulted in a significant decrease in the calculated rate coefficients, and failure to fit the observed data. A direct, barrierless, bond-insertion process is not therefore a viable mechanism for removal of Ta clusters with the alkanes studied here, because it requires a much tighter transition state in the model that does not fit the data. We conclude that a rate-determining molecular association step best characterizes these Ta cluster/alkane reactions.

We calculate a range of entropy changes associated with transition state formation from -111 J K^{-1} mol^{-1} (Ta atom + *n*-butane) to -73 J K^{-1} mol^{-1} (Ta_{30} + isobutane). Table 2 summarizes the range of values calculated, with values of higher magnitude being invariably associated with the atom and small clusters, and lower magnitude values being associated with larger clusters. These values show the loss of entropy involved formation of an association complex with significant internal degrees of freedom, a loss that is alone sufficient to account for a 3 order-of-magnitude drop in the rate coefficients with respect to the anticipated collision rate constant. At the temperatures at which our experiments were carried out, such entropy changes give rise to contributions to the Gibbs free energy of the order of 20−30 kJ mol^{-1} at the temperature of our reactions (300 K). Thus, these "barrierless" complex formation processes exhibit a significant Gibbs free energy barrier to reaction entirely due to entropic constraints on the reaction process.

The results of the present study are in remarkable accord with known behavior of hydrocarbons on surfaces.[22−25] Hydrocarbons larger than methane are among the small group of species that are known to adsorb on metal surfaces by a nonactivated process. Ehrlich[22] has reviewed early work until the later 1980s on the subject of activated chemisorption and includes in this work a summary of nonactivated adsorption of hydrocarbons. Such species show a nonzero sticking probability at very low temperatures that initially *decreases* as the translational energy of the hydrocarbon is increased. Such behavior is characteristic of the formation of a precursor state via a nonactivated step, prior to any steps that involve activated rearrangement processes. More recent work, including low-incident kinetic energy molecular beam studies by the Madix group,[23,24] support this conclusion strongly. Adsorption of hydrocarbons via a three-center, two-electron interaction with metal centers appears to be the norm, because activation energies observed for subsequent dissociative adsorption are typically much lower than the strength of a typical C−H bond.[25] Zaera[25] points out that formation of such centers of interaction is controlled by entropic factors, resulting in a low probability of reaction at all temperatures. Thus, the importance of a nonactivated, entropically controlled initial step in surface-mediated hydrocarbon reforming is well documented.

In many ways, hydrocarbons larger than methane are an ideal family of molecules to use in the study of entropy-derived effects on rate parameters and other aspects of dynamics and reactivity. The presence of any exoergic reaction route during the initial interaction of a molecule with a cluster or a surface masks the importance of entropy effects, relegating them to the role of often-invisible moderators of the magnitude of the free-energy change associated with the process in question. In hydrocarbon studies no highly exoergic interactions are possible in the initial stages of reaction, the influence of entropy may be clearly seen, and its importance can be recognized.

D. Metal Clusters as Models for Hydrocarbon Reaction Processes on Surfaces. Our observation that the alkanes studied here react via an entropy-controlled nonactivated process to yield a molecularly adsorbed product in the rate-determining step is entirely in accord with results from surface studies summarized above. Notable is our ability to model the rate coefficients in the context of a transition state involving a flexible, local interaction between one contact point on the hydrocarbon and a metal site, which is in accord with the C−H···M, two-electron interaction model that is believed to characterize the interaction of alkanes with surfaces prior to any bond cleavage or isomerization.[25] Also, our inability to measure a rate for methane-mediated removal of Ta clusters is in accord with the exceptional nature of methane with respect to other alkanes, a singular character that is due to the spherical nature of the methane molecule and the inaccessibility of its C−H bonds for side-on interaction.[22] Finally, the importance of entropy in dominating the adsorption rate for molecular species for which there is no favorable enthalpy-driven process is clearly underscored in our work.

E. Dependence of Cluster Size Selectivity on the Nature of the Reagent. Due to the relatively weak interactions involved in association complex bonding, formation of such complexes is expected to be much less sensitive to cluster geometric structure and the availability of suitable multiatom reaction sites, which may vary with cluster size. Accordingly, the reaction rates for cluster removal by association complex formation is not expected to fluctuate erratically as a function of cluster size, as observed. Also, association complex formation in a barrierless (nonactivated) reaction implies product states that can be directly accessed by the neutral ground states of the cluster and alkane. In contrast, dissociative chemisorption reactions, as exemplified by $Nb_n + H_2$, where barriers are associated with curve crossings involving states that correlate to ionic or electronically excited states of the reactants, can be highly sensitive to the metal cluster electronic structure. However, the presence of molecular association complex formation as a first step to cluster reaction does not preclude size-selective chemistry from taking place on early transition metal clusters. Rather, these cases imply only that the rate-determining step for cluster removal is most consistent with molecular adsorption, which is a structurally

insensitive process. Subsequent steps in the mechanism, including those involving bond cleavage, insertion, and formation, are expected to be highly cluster-size sensitive. This fact is reflected in the significant variations in the extent of dehydrogenation with cluster size previously reported for Nb cluster reactions with isobutane.[3] Such an observation implies that sensitivity of the product distributions to the cluster size may be observed that is not reflected correspondingly in the rate of cluster removal. This is a key observation in terms of understanding the anomalous absence of selectivity in the kinetics of transition metal cluster reactions with larger molecules.

Our analysis indicates that it is the degree of irreversibility of the initial formation of an association complex that determines whether a reaction will exhibit cluster-size selectivity. When the complexation process is irreversible, the observed rate coefficient is simply that for a barrierless association process, the characteristics of which are determined by the appropriate transition state for molecular adsorption (TS1, Figure 1). Such a process is expected to show little sensitivity to the details of the cluster geometry and electronic structure. This situation is expected to apply for large molecules, for which higher polarizabilities and more numerous dative interactions with the cluster surface are possible. In addition, any small molecules that can bind very strongly to the cluster in a manner that does not involve ligand bond cleavage should show this behavior. Indeed, reactions of CO with several transition metal clusters are known to show nonsize selective chemistry reminiscent of the alkane rate coefficient data presented here.[13]

Small molecules and those not normally thought of as strong coordinating ligands, such as H_2, and N_2, for which selectivity is commonly observed,[1,6−16] are expected to form much weaker association complexes, involving less dative bond formation in the precursor complex. This should be augmented by lower physisorption energies associated with their decreased polarizability. Such ligands would then be expected to form association complexes of modest binding energies. These weakly bonded precursors may then dissociate or proceed through the transition state to dissociative chemisorption. In this case, the rate expression would show explicit dependence on the magnitude of the energy barrier to dissociative chemisorption (TS2, Figure 1), which is expected to vary significantly with the cluster size. Such variation would reflect changes in cluster geometric and electronic structure that have a direct impact on the magnitude of the barrier to chemisorption, and hence the kinetics observed in this regime. Therefore, it is clear that a unified view of the metal cluster reaction potential energy surfaces is entirely consistent with both the observation of profound variations in the rate coefficients with cluster size for cluster depletion by weakly associative molecules, and the much more modest cluster size dependence observed for analogous processes involving strongly associative molecules.

F. Anomalous Reactivity of Ta_{11} and Other Ta Clutsers. Finally, the anomalous reactivity of Ta_{11} (and to a much lesser extent Ta_{23} and Ta_{27}) is exceptional with respect to this model and suggests that a somewhat different mechanism is active in the reactions of this cluster with hydrocarbons. The most likely explanation is that the bond-cleavage steps that follow complexation of the hydrocarbon begin to occur much earlier on the reaction coordinate for these clusters, such that the entropy-derived Gibbs free energy lost in localizing the hydrocarbon on the cluster surface is countered by enthalpically derived Gibbs free energy gains associated with new covalent bond formation. This result would suggest that Ta_{11} in particular has an unusual propensity for reaction with hydrocarbons and holds some promise as an alkane activation center in cluster-size specific catalysis.

V. Summary and Conclusions

A smooth, near-monotonic increase in the rate coefficients, as a function of the number of Ta atoms per cluster, is a characteristic feature of the reactions of Ta clusters with ethane, propane, *n*-butane, isobutane, and neopentane. Exceptions are the anomalously high reactivity of Ta_{11} with all alkanes studied having secondary or tertiary C−H bonds, and very small clusters. Despite the loose nature of the transition states involved in these systems, the rates of reaction are limited to values well below the collision rate by entropic constraints. The loss of entropy associated with localizing relatively large reagents, like alkanes, onto the surface of a cluster accounts for the 2−3 order of magnitude difference between the collision rate and the actual rate of reaction.

The relatively loose nature of the transition state indicates that the formation of a molecularly bound association complex is the initial step in the reaction. The nature of the potential energy surface associated with this reaction provides an explanation as to why some metal cluster reactions show large oscillations in reactivity with cluster size, whereas others, as typified by the Ta_n/alkane reactions reported here, do not. Association complex formation can be expected to be less sensitive than dissociative chemisorption to cluster size and the associated variations in electronic and geometric structure. When such complex formation constitutes the rate-determining step, subsequent selectivity in the chemistry is effectively masked. Cluster size selectivity is not expected for cluster reactions involving strongly bound association complexes (i.e., with large hydrocarbons, strongly coordinating ligands). It is, however, expected for reactions that occur with small or weakly coordinating molecules, for which the entropy loss on association complex formation is relatively small.

It is important to note that the absence of cluster size selectivity observed in the kinetics measurements discussed here by no means implies that the overall chemistry does not vary dramatically with cluster size. It is a drawback of cluster depletion kinetics measurements that they focus on the rate-determining step and do not reflect any of the subsequent chemistry beyond the transition state. We must therefore look beyond such kinetics to explore the intimate details of such reactions, especially where larger molecules are concerned. We are currently investigating analysis of product distributions as an alternative approach.

Supporting Information Available: The manner in which the various partition functions were calculated for the transition state model is described in detail in the Supporting Information. This material is available free of charge via the Internet at http://pubs.acs.org.

References and Notes

(1) Berces, A.; Hackett, P. A.; Lian, L.; Mitchell, S. A.; Rayner, D. M. *J. Chem. Phys.* **1998**, *108*, 5476.

(2) Knickelbein, M. B. *Annu. Rev. Phys. Chem.* **1999**, *50*, 79.

(3) Lafleur, R. D.; Parnis, J. M.; Rayner, D. M. *J. Chem. Phys.* **1996**, *105*, 3551.

(4) See, for example: Hudson, J. B. *Surface Science An Introduction*; Wiley: New York, 1998.

(5) Pitt, I. C.; Gilbert, R. G.; Ryan, K. R. *J. Phys. Chem.* **1994**, *98*, 13001.

(6) Holmgren, L.; Andersson, M.; Rosen A. *J. Chem. Phys.* **1998**, *109*, 3232.

(7) Ho, J.; Parks, E. K.; Riley, S. J. *J. Chem. Phys.* **1993**, *99*, 140.
(8) Nonose, S.; Sone, Y.; Kikuchi, K.; Fuke, K.; Kaya, K. *Chem. Phys. Lett* **1989**, *158*, 152.
(9) Hamrick, Y. M.; Morse, M. D. *J. Phys. Chem.* **1989**, *93*, 6494.
(10) Parks, E. K.; Riley, S. J. *Proceedings of the International School of Physics*; North-Holland: Amsterdam, 1988.
(11) Richtsmeier, S. C.; Parks, E. K.; Liu, K.; Pobo, L. G.; Riley, S. J. *J. Chem. Phys.* **1985**, *82*, 3659.
(12) Mitchell, S. A.; Lian, L.; Rayner, D. M.; Hackett, P. A. *J. Chem. Phys.* **1995**,*103*, 5539.
(13) Morse, M. D.; Geusic, M. E.; Heath, J. R.; Smalley, R. E. *J. Chem. Phys.* **1985**, *583*, 2293.
(14) Parks, E. K.; Nieman, G. C.; Riley, S. J. *J. Chem. Phys.***1996**, *104*, 3531.
(15) Mitchell, S. A.; Rayner, D. M.; Bartlett, T. A.; Hackett, P. A. *J. Chem. Phys.* **1996**, *104*, 4012.
(16) Cox, D. M.; Reichmann, K. C.; Trevor, D. J.; Kaldor, A. *J. Chem. Phys.* **1998**, *88*, 111.
(17) Pedersen, D. B.; Parnis, J. M.; Lafleur, R. D.; Rayner, D. M. *J. Chem. Phys.* **1998**, *109*, 551.
(18) Note that, given that the ionization potential of a Ta atom is greater than the energy of one photon at 193 nm, the observation of Ta atoms in our mass spectra must correspond to photoionization of electronically excited atoms. We do not feel that such excitation will influence the observed kinetics significantly, unless bond cleavage and isomerization processes are involved.
(19) Berg, C.; Kaiser, S.; Schindler, T.; Kronseder, C.; Nieder-Schattburg, G.; Bondeybev, V. E. *Chem. Phys. Lett.* **1994**, *231***,** 139.
(20) Collings, B. A.; Rayner, D. M.; Hackett, P. A. *Int. J. Mass. Spectrom. Ion Processes* **1993**, *125***,** 207.
(21) See Supporting Information for details of the transition state modelling procedure.
(22) Ehrlich, G. In Chemistry and Physics of Solid Surfaces VII; Vanselow, R., Howe, R. F., Eds.; Springer-Verlag: New York, 1988; Chapter 1.
(23) Soulen, S.A.; Madix, R. J. *Surf, Sci.* **1995**, *323*, 1.
(24) Hamza, A. V.; Steinruck, H.-P., Madix, R. J. *J. Chem. Phys.* **1987**, *86*, 6506.
(25) Zaera, F. *Appl. Catal. A.* **2002**, *229*, 75.